

Low Temperature Properties of Finite Dimensional Ising Spin Glasses: (some) Numerical Simulations

Juan J. Ruiz-Lorenzo

Departamento de Física, Facultad de Ciencias, Universidad de Extremadura.

Avda Elvas s/n. 06071 Badajoz. Spain.

and

Instituto de Biocomputación y Física de Sistemas Complejos.

Universidad de Zaragoza. 50009 Zaragoza, Spain.

ruiz@unex.es

21 April 2003

Abstract

We review some recent results on finite dimensional spin glasses by studying recent numerical simulations and their relationship with experiments. In particular we will show results obtained at zero and non zero temperature, focusing in the low temperature properties of the model, and contrast them with different pictures of the low temperature phase of spin glasses: Replica Symmetry Breaking, Droplet Model and Trivial-Not-Trivial Scenario.

1 Introduction

Spin glasses are still a problematic issue. The introduction of frustration and disorder in a statistical model has posed a real challenge to both experimentalist and theoreticians.

One can take, as an example, the “canonical spin glass”: a metal (*e.g.* Copper) in which ferromagnetic impurities have been introduced (*e.g.* Manganese). This system can be studied in the RKKY framework and the result is an oscillating interaction which couples the magnetic moments of the material. This oscillatory behavior induced by the disorder (magnetic moments) also introduces frustration in the material [1].

In this work, given the limitations of space, we have restricted ourselves to treating a few topics related to numerical simulations in finite dimensional spin glasses (only on Ising like models), focusing on the properties of the low temperature phase, yet we will treat them in detail. In the last years, a large amount of work on finite temperature numerical simulations but also zero temperature ones and experiments have been done. We will try to give a detailed description of some of these simulations and experiments, highlighting common observables in them and contrasting these results with some of the three main theoretical models: Droplet Model (DM) [2], TNT (Trivial overlap but Not Trivial link overlap) [3, 4] and Replica Symmetry Breaking (RSB) [5, 6, 7]. Related work can be found in [8].

Unfortunately, we have put aside in this work interesting studies on rheology [9, 10], ultrametricity [11, 12, 13], Heisenberg spin glasses [14, 15], suitability of the Edwards-Anderson model to describe real experiments [16], two dimensional Ising spin glasses [17, 18], heterogeneity [19, 20, 21, 22], Sherrington-Kirkpatrick model [23, 24], sum rules [7], anisotropy [25], chaos [26, 27, 28, 29], eigenvalues analysis [30], three dimensional ferromagnetic spin glasses [31] and in field numerical simulations [32, 33, 34, 35]. The list of references given in this paragraph is not complete.

Very good reviews and books have been written in the past years. We refer the reader to them [36, 37, 6, 1]. In addition numerical simulations have been reviewed in [39, 38], experiments in [40] and dynamics in [41, 42, 43, 44].

To put this work into context we will review (briefly) the three main theoretical approaches to spin glasses.

The first one is the so-called Replica Symmetry Breaking. It is based in the standard procedure which has worked extremely well in Statistical Mechanics in the past decades (the paradigm is the ordered Ising model). Firstly, one must solve the model in the Mean Field approximation. This is equivalent to solve the infinite dimensional model exactly. This was done by G. Parisi in 1980 [5, 6]. His main results are that there exist a (countable) infinite number of (finite volume) pure states organized in an ultrametric fashion. The differences in extensive free energy among these pure states are of order one. In addition, the interface between two of these states is space filling (its surface scales as its volume, like an sponge) [7]. The Parisi solution also predicts a transition in magnetic field.

Once we know which is the solution in infinite dimensions (where there are no fluctuations) we enable the system to fluctuate around the Mean Field solution (in this case, that of Parisi). The appropriate technique to handle this kind of problem is the Renormalization group (that can be implemented in the Field Theoretical approach) and the goals are computing the upper critical dimensions (above which Mean Field provides a good picture of the transition) and determining the critical exponents (at fixed dimension or in the ϵ -expansion) below the upper critical

dimension. Within this approach it is very difficult (since it is based mainly in perturbation theory) to estimate the lower critical dimension (the largest dimension below which there is not phase transition). The renormalization group program has been done (in part) by de Dominicis, Temesvari and Kondor [45]. We should remark that this approach does not change the low temperature properties. Hence in between the lower critical and infinite dimensions the qualitative description of the broken phase is still provided by the Parisi solution.

Another compelling theory is the droplet model [2]. The rationale of this model is the Migdal-Kadanoff renormalization group. This technique is exact in one dimension and is approximate in higher dimensions. The main results of the DM is that there are two pure states (only one, if we consider the global spin flip symmetry), and that the magnetic field destroys the phase transition. In addition we can mention that the typical excitations are compact domains of reversed (against the ground state) spins. The cost in energy of these excitations scales as a power of the typical size of the droplet, L^θ .

Recently has been proposed a third way which interpolates between the droplet model and RSB: the TNT proposal [3, 4]. In RSB $\theta = 0$, since we can create an excited state with $\mathcal{O}(1)$ energy. In this third approach $\theta = 0$ as in RSB but the link overlap is trivial (as in the droplet model: the probability distribution of the link overlap is delta peaked). In RSB the link overlap is believed to be proportional to the squared of the overlap (in infinite dimension the link overlap $q_l = q^2$, where q is the overlap): as far as the probability distribution of the overlap is not trivial then the probability distribution of the link overlap must not be delta peaked. We refer the reader to the text below for more details about the link overlap.

The chapter is organized as follows. In the first section we examine the issue of the phase transition, giving strong numerical results which support a finite transition at non zero temperature. Next we will study the properties of the low temperature region (below the critical point). In this part we show numerical simulations which highlight physical properties which can be described consistently assuming a RSB phase. Moreover we will describe the experimental computation of the dynamical correlation length and the possible interpretations of the different scalings proposed. In section 4 we will study the generalization of the fluctuation dissipation theorem out of equilibrium, starting with the analytical basis and continuing with some numerical results which support the link statics-dynamics. This tool is very important because it can be implemented in experiments (we will show these). In section 5 we will show the memory/rejuvenations experiments. In the following section we will study zero temperature properties which probe the different theoretical pictures. Finally we will return to non zero temperature and describe recent numerical simulations computing the link overlap at finite temperature.

2 On the phase transition

This part of the review is devoted to showing numerical evidences which favor strongly a phase transition in the three dimensional Ising spin glass at finite temperature.

The existence of a phase transition in the three dimensional Ising spin glass has been attacked mainly using finite size scaling (FSS) methods [46]. In these methods one monitors which is the behavior of some (critical) observables of the system when one changes the size of it. We will describe in this section how to implementate the FSS to spin glasses and then how to define a good cumulant which signs clearly the transition point.

The initial point is to introduce the Edwards-Anderson Hamiltonian [47]

$$\mathcal{H} = - \sum_{\langle i,j \rangle} J_{ij} \sigma_i \sigma_j , \quad (1)$$

where the sum is extended to all the pairs of nearest neighbors, $\sigma_i = \pm 1$ are Ising variables and J_{ij} are random (quenched) variables. In general the J_{ij} are drawn for a Gaussian distribution with zero mean and unit variance. One can also choose the random couplings from a bimodal distribution: $J_{ij} = \pm 1$ with equal probability.

It is well known that observables in spin-glasses need to be defined in terms of real replicas, that is, for every disorder realization, one considers two thermally independent copies of the system $\{\sigma_i, \tau_i\}$ [39]. Observables are most easily defined in terms of a spin-like field, the so-called overlap field (which is the order parameter in spin glasses):

$$q_i = \sigma_i \tau_i . \quad (2)$$

The total overlap is the lattice average of the q_i

$$q = \frac{1}{V} \sum_i q_i , \quad (3)$$

while the (non-connected) spin-glass susceptibility is¹

$$\chi_q = V \overline{\langle q^2 \rangle} . \quad (4)$$

In Finite-Size Scaling studies, it is useful to have dimensionless quantities, that go to a constant value at the critical temperature. The standard example of this quantity is the Binder cumulant

$$g_4 = \frac{3}{2} - \frac{1}{2} \frac{\overline{\langle q^4 \rangle}}{\overline{\langle q^2 \rangle}^2} . \quad (5)$$

¹As usual we use the brackets to denote the thermal average for a given choice of disorder, and the overline to mark the average over the disorder.

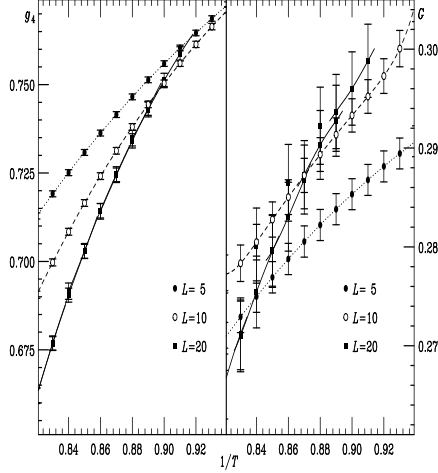


Figure 1: g_4 and G cumulants as a function of the inverse temperature for the three dimensional $\pm J$ Ising spin glass [50].

Another example is the g_2 cumulant [48], that measures the lack of self-averageness of the spin-glass susceptibility

$$g_2 = \frac{\overline{\langle q^2 \rangle^2} - \overline{\langle q^2 \rangle}^2}{\overline{\langle q^2 \rangle}^2} . \quad (6)$$

In reference [51] a third cumulant was proposed which is a function of g_4 and g_2

$$G = \frac{1}{2} \frac{g_2}{1 - g_4} . \quad (7)$$

These cumulants have been really useful to characterize phase transitions both in ordered systems (the Binder cumulant) and in disordered ones (g_2 in diluted Ising models). Nevertheless in Ising spin glasses they do not provide a clear signature of the phase transition (*i.e.*, a clear crossing between curves corresponding to different lattice sizes). In Figure 1 we show both cumulants as a function of the temperature for the three dimensional Ising model (with a binomial distribution for the couplings and helicoidal boundary conditions).

Unfortunately, g_4 and g_2 require the evaluation of a four-point correlation function, which is statistically a much noisier quantity than a two-point one. A more convenient observable is the correlation-length, which is defined only in terms of the two-point correlation function. Notice that its ratio with the lattice size is

again dimensionless [46]. We therefore are faced with the problem of defining a correlation-length on a finite lattice. This was done in Ref. [49]. The main steps of the constructions are the following. Let $C(\mathbf{r})$ be the correlation function of the overlap field,

$$C(\mathbf{r}) = \frac{1}{V} \sum_i \overline{\langle q_i q_{i+\mathbf{r}} \rangle} \quad (8)$$

and $\hat{C}(\mathbf{k})$ its Fourier transform. Notice that $\hat{C}(0)$ is the spin glass susceptibility. Then, inside the critical region on the paramagnetic side and in the thermodynamical limit, one has

$$\hat{C}(\mathbf{k}) \propto \frac{1}{k^2 + \xi^{-2}}, \quad \|\mathbf{k}\| \ll \xi^{-1}, \quad (9)$$

$$\xi^{-2} = -\frac{1}{\hat{C}} \frac{\partial \hat{C}}{\partial k^2} \bigg|_{\mathbf{k}^2=0}. \quad (10)$$

On a finite lattice, the momentum is discretized, and one uses [49] a finite-differences approximation to eq. (10),

$$\xi^2 = \frac{1}{4 [\sin^2(k_m^x/2) + \sin^2(k_m^y/2) + \sin^2(k_m^z/2)]} \left[\frac{\chi_q}{\hat{C}(k_m)} - 1 \right], \quad (11)$$

where χ_q was defined in eq. (4) and k_m is the minimum wave-vector allowed for the boundary conditions used (e.g., $\mathbf{k}_m = (2\pi/L, 2\pi/L^2, 2\pi/L^3)$ for helicoidal boundary conditions). Of course, eq. (10) holds in the thermodynamic limit ($L \gg \xi$) of the paramagnetic phase. As we do not use connected correlation functions, ξ has sense as a correlation length only for² $T > T_c$.

We can study the scaling behavior of the finite-lattice definition (11) on a critical point, where the correlation function decays (in d dimensions) as $r^{-(d-2+\eta)}$. The behavior of the Fourier transform of the correlation function for large L in three dimensions is given by

$$\hat{C}(k) \sim \int_0^L dr r^{1-\eta} \frac{\sin(kr)}{kr} \quad (12)$$

and one finds that $\chi_q/\hat{C}(k_m)$ goes to a constant value, larger than unity, because $\|\mathbf{k}_m\| = \mathcal{O}(1/L)$. Furthermore, ξ/L tends to a universal constant at a critical point (like the Binder cumulant g_4). Moreover, on a broken-symmetry phase, where the fluctuations of the order parameter are not critical, one has $\chi_q = \mathcal{O}(L^d)$, while

²We use T_c to denote the critical temperature obtained in numerical simulations and in theoretical computations and T_g the one obtained in experiments.

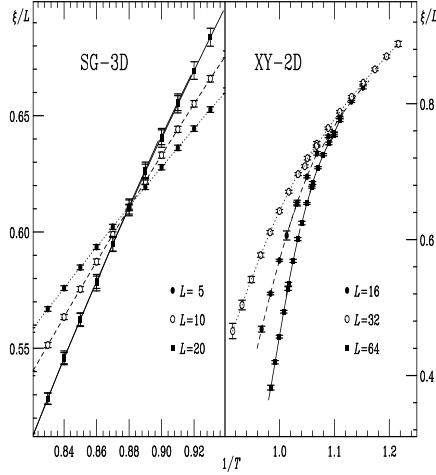


Figure 2: ξ/L cumulant for the three dimensional $\pm J$ Ising spin glass (left part of the figure). The same plot for the two dimensional XY (ordered) model. Taken from reference [50].

$\hat{C}(k_m) = \mathcal{O}(1)$. Therefore the full description of the scaling behavior of ξ/L is as follows. Let ξ_∞ be the correlation-length in the infinite lattice: in the paramagnetic phase, for $L \gg \xi_\infty$, one has $\xi/L = \mathcal{O}(1/L)$. In the scaling region, where $\xi_\infty \geq L$, $\xi/L = \mathcal{O}(1)$, while in a broken-symmetry phase on a lattice larger than the scale of the fluctuations, $\xi/L = \mathcal{O}(L^{d/2})$. Consequently, if one plots ξ/L for several lattice sizes as a function of temperature, the different graphs will cross at the critical one.

We can see the (clear) crossing phenomena in Figure 2. Also shown in this figure (right part) the same observable for the two dimensional XY model (with no disorder). This double plot tells us that 1) there is a phase transition at a finite temperature and 2) we should discard $T_c = 0$ and XY-like scenarios for the phase transition of the three dimensional Ising spin glass ³.

3 Some properties of the low temperature region

In this section we will describe numerical simulations and experiments which try to discern which are the low temperature properties of the three dimensional Ising spin glass by working well below the transition point. We will start by discussing

³These numerical results have been obtained with the dedicated computer SUE [52], which has a performance of 0.2 ns/spin.

the properties at the upper critical dimension of the model (which is six) where the analytical predictions from RSB simplify. Then we will report results in three dimensions. Finally we will review some issues related to the behavior of the dynamical correlation length.

3.1 $d = 6$

First, we will check one of the RSB predictions. To do this, numerical work has been carried out just at the upper critical dimension. In this dimension there is no renormalization of the powers of propagators (*i.e.*, the anomalous dimension vanishes) and only multiplicative factors occur⁴.

If RSB holds, a $1/p^4$ propagator should be found by looking at the $q = 0$ sector of the model in the broken phase ($T < T_c$)⁵. We remark that at six dimensions the equilibrium overlap-overlap correlation function constraint to $q = 0$ was obtained by De Dominicis *et al.* [45]

$$C_{\text{RSB}}(x)|_{q=0} \sim \begin{cases} x^{-4} & \text{if } T = T_c, \\ x^{-2} & \text{if } T < T_c, \end{cases} \quad (13)$$

which corresponds to $1/p^2$ at $T = T_c$ (the usual critical propagator) and $1/p^4$ (the replicon mode) for $T < T_c$.

From this correlation function we can compute the associated (spin glass) susceptibility

$$\chi = \int d^6x C(x). \quad (14)$$

Since we are working on a finite lattice, the previous integral must be performed in a box of size L . If we want to observe the dynamical behavior of χ , the upper limit in the integral should be changed to $\xi(t)$, the dynamical correlation length. At this point we can assume that $\xi(t) \simeq t^{1/z(T)}$, which defines an, in principle, effective dynamical critical exponent, $z(T)$. Furthermore, one can assume a functional dependence $z(T) = 4T_c/T$, where T_c is the critical temperature: with this temperature dependence we recover the value z at the critical temperature $z(T_c) = 4$ as predicted by Mean Field [6]. The result for $\chi(t)$ is

$$\chi(t) \sim \begin{cases} t^{1/2} & \text{if } T = T_c, \\ t^{4/z(T)} & \text{if } T < T_c. \end{cases} \quad (15)$$

⁴At the upper critical dimension logarithmic corrections appear. These have been studied numerically by Wang and Young [53], and subsequently computed analytically in reference [54].

⁵This ergodic sector is very important. Out of equilibrium, the system remains in this sector.

This expression can be compactly written as

$$\chi(t) \sim t^{h(T)} . \quad (16)$$

This formula should be valid if we remain all the time in the $q = 0$ sector. Hence, the exponent $h(T)$ is a discontinuous function of temperature: *i.e.*, $h(T_c^-) = 1$ while $h(T_c^+) = 1/2$. Moreover $h(T)$, if the Ansatz for $z(T)$ is right, should grow linear.

This can be tested by performing an out of equilibrium numerical simulation in a large lattice. The run starts at random and suddenly the system is quenched below the critical temperature. At this point the growth of the non linear susceptibility is recorded. At the same time, one can check that the system (due to the large lattice simulated) develops no overlap (and so we are sure that we are simulating inside the $q = 0$ sector of the theory). The strategy is to point out the discontinuity of the power of the $q = 0$ propagator when we reach the critical temperature from below (the propagator changes from $1/p^4$ to the standard and critical $1/p^2$ propagator). So, one needs to redo the previous schedule but quenching to the critical temperature.

In Figure 3 we plot the results and it is clear that the system behaves as RSB predicts: $h(T)$ grows linear below the critical point and develops a discontinuity, just on the amount predicted by RSB, at the critical temperature. And so, it has been shown 1) the existence of the replicon mode at finite dimensions and 2) the growth of the correlation length can be described with the following law: $\xi(T, t) \simeq t^{1/z(T)}$ with $z(T) \propto 1/T$ [55].

The next step is trying to see if this picture holds in lower dimensions, in particular in the physical dimension three.

3.2 $d = 3$

In three dimensions, it is possible to handle this problem (replicon mode in addition to a given behavior of $\xi(t, T)$) by studying the decay with time and position of the overlap-overlap correlation function,

$$C(x, t) = \frac{1}{L^3} \sum_i \overline{\langle \sigma_{i+x} \tau_{i+x} \sigma_i \tau_i \rangle_t} . \quad (17)$$

where σ and τ are two real replicas (which evolve with the same disorder) and the index i runs over all the points of the lattice. As usual we denote by $\overline{(\dots)}$ the average over the disorder and, in this context, $\langle \langle \dots \rangle \rangle_t$ is the average over the dynamical process (for a given realization of the disorder) at time t . In plain words, the two replicas (σ and τ) evolve with the same disorder but with different random numbers.

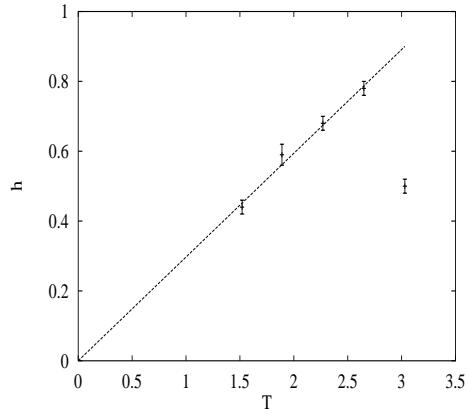


Figure 3: Susceptibility exponent as a function of the temperature in the six dimensional Ising spin glass [55]. Notice the linear region below the critical temperature and the discontinuity at the critical point.

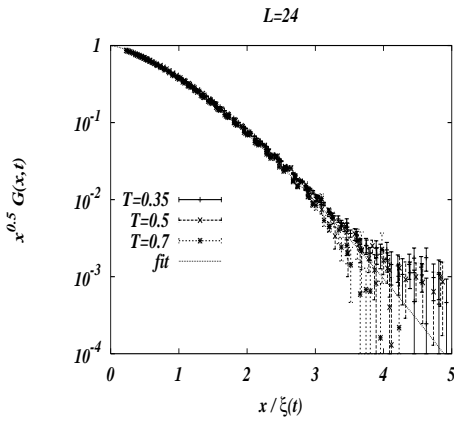


Figure 4: Re-scaled correlation function, $x^\alpha C(x, t)$, against the scaling variable, $x/t^{1/z}$, for $L = 24$ and $T = 0.35, 0.5$ and 0.7 . Taken from reference [74]. Notice the quality of the scaling.

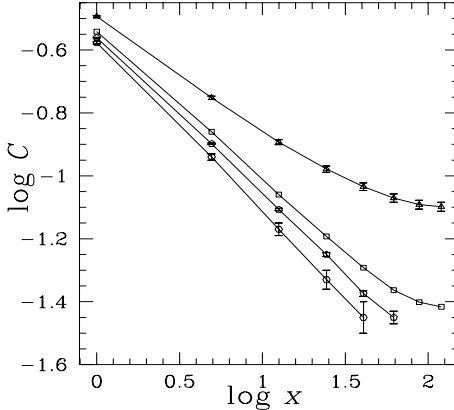


Figure 5: We show four overlap-overlap correlations functions at $T = 0.7$. From top to bottom: 1) equilibrium correlation function, 2) equilibrium (but computed with a small cut-off on the overlap) correlation function 3) and 4) extrapolation to infinite time of two dynamical correlation functions computed using two different annealing procedures. See the text for more details. Figure taken from reference [57].

In the $q = 0$ sector (obtained simulating very large lattices, for large times, but by controlling that the overlap of the system is always very small) it has been obtained that the numerical data [58, 74] follow very well the following scaling law (it has been checked that this behavior also holds in four dimensions [56, 60])

$$C(x, t) = \frac{1}{x^\alpha} \exp \left[- \left(\frac{x}{\xi(t)} \right)^\delta \right]. \quad (18)$$

We show in Figure 4 the scaling plot for three different temperatures and the fit using eq. (18). The scaling plot and the agreement with the fit is very good. We can cite that the α exponent does not show a clear temperature dependence in three dimension ($\alpha \simeq 0.5$) [58, 74]⁶, whereas in four dimension the situation is very different since the alpha exponent varies greatly with temperature [56, 60].

This scaling law provides us with the equilibrium form of the propagator, by taking the limit $t \rightarrow \infty$ in eq. (18):

$$C_{\text{eq}}(x) \equiv \lim_{t \rightarrow \infty} C(x, t) \propto \frac{1}{x^\alpha}, \quad (19)$$

⁶In three dimensions [87] it has been found at zero temperature that $\alpha \simeq 0.4$, in good agreement with the value found at non zero temperature.

where the proportionally constant is $C_{\text{eq}}(x = 1)$. Of course, the exponent is not as found in six dimensions due to the renomalization effects (see eq. (13)).

A further test can be done in three dimensions in order to check the pure power law of the correlation function restricted to small overlaps, eq. (19). One can compare this behavior (obtained dynamically and using an extrapolation) with that obtained by computing at equilibrium the overlap-overlap correlation function by taking only those measures with overlap $q < 0.01$. In Figure 5 we plot in the lower part of the figure two curves corresponding to the correlation function obtained in a dynamical process taking the extrapolation to infinite time. The upper curve is the equilibrium correlation function (computed without imposing cut-off) and finally the last curve is the equilibrium one computed using a small cutoff ($q_{\text{max}} = 0.01$). The agreement between the lower three curves is really good. This plot provides an additional evidence to the existence of a replicon mode in three dimensions [57]. In the droplet model $C_{\text{eq}}(x) \rightarrow q_{\text{EA}}^2$ as $x \rightarrow \infty$ in contrast with the numerical results which support eq. (19).

3.3 Dynamical correlation length

We have seen that in six dimensions the correlation length can be fitted $\xi(T, t)$ as $t^{1/z(T)}$ with $z(T) = z_c T_c / T$, where z_c is the dynamical critical exponent at the critical point (T_c). In particular, it was found in three dimensions that [58, 74, 59, 38]

$$\xi(t, T) \propto t^{0.153(12)T/T_c}, \quad (20)$$

where we have assumed that $T_c = 0.95(3)$. In four dimensions [56] a similar behavior was found

$$\xi(t, T) \propto t^{0.19(1)T/T_c}, \quad (21)$$

where $T_c = 1.80(1)$. The behavior in four dimensions interpolates very well between the three dimensional results and that obtained in six dimensions $\xi(t, T) \propto t^{0.25T/T_c}$.

This dependence of the dynamical correlation length with temperature and time has been checked experimentally. The basic idea of the experiment reported in reference [61], was to introduce an external magnetic field and then operationally define the dynamical correlation length via the volume of the droplet which contributes to the Zeeman energy: $E_{\text{Zeeman}} \propto N_s \chi H^2$ (where N_s is the number of spins contributing to the Zeeman energy, H is the magnetic field and χ is the magnetic susceptibility). By effect of the magnetic field, the typical times of the dynamics are modified by a factor $\exp(-cN_s \chi H^2/T)$, where c is a numerical factor. By measuring this reduction factor one can extract the number of spins involved in the dynamics for a given waiting time and temperature and using that $N_s \propto \xi(t_w, T)^3$,

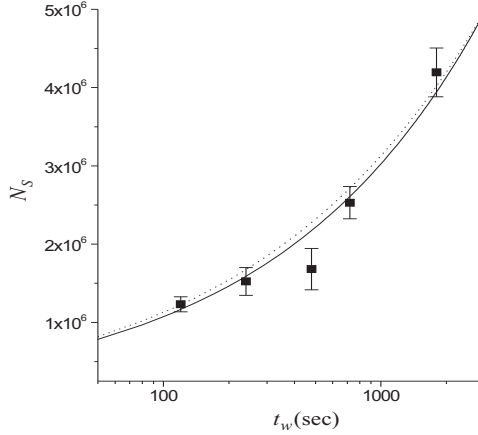


Figure 6: N_s , number of spins participating in barrier quenching (and hopping) as a function of $\log t_w$ at $T = 0.78T_g = 28$ K for CuMn. The solid curve is the prediction for power law dynamics, while the dashed one comes from activated dynamics, see the text for more details. Taken from reference [61].

$\xi(t_w, T)$ can be computed. In this way they computed the correlation length and by performing the experiment at different temperatures. The following experimental dependence was found (see the solid line in Figure 6):

$$\xi(t_w, T) = 0.653 \left(\frac{t_w}{\tau_0} \right)^{0.169T/T_g}, \quad (22)$$

where $1/\tau_0 = 4.1 \times 10^{12} \text{ s}^{-1}$. The agreement with the result obtained in numerical simulations (see eq. (20)) is very good. Nevertheless a fit assuming activated dynamics (droplet model) is also possible (see the dashed line in Figure 6), obtaining

$$\xi(t, T) = 10^{-5} \left[\frac{T}{T_g} \log \left(\frac{t_w}{\tau_0} \right) \right]^{\frac{1}{0.21}}. \quad (23)$$

However we see that the prefactor of the fit is really small (it would be natural for it to be $\mathcal{O}(1)$). Moreover the ψ exponent is just at the lowest allowable value in the droplet model ($\psi = 0.2$). However, numerical work suggests that $1/\psi = 1/0.7$ [59, 38].

A plausibility argument for the linear dependence of the effective dynamical critical exponent $z(T)$ with the inverse of the temperature was given by H. Rieger in reference [38]. Assuming an Arrhenius law and that free energy barrier for an

excitation of typical size L , scales as $\log L$ (*i.e.*, $\psi = 0$), we can obtain that⁷

$$\tau \propto \exp \left(c \frac{\log L}{k_B T} \right), \quad (24)$$

where c is a constant, which can be rewritten as $\tau \propto L^{1/z(T)}$ with $z(T) \propto 1/T$.

However, a different argument based in the droplet picture and also accounting for the experimental data can be given [62]. Indeed, let us assume that the time needed to evolve a conformation on a scale of size l_n is given by (this defines the ψ droplet exponent)⁸

$$t_n = t(l_n) \sim \tau_0 \exp \left(\frac{\Upsilon l_n^\psi}{k_B T} \right). \quad (25)$$

This behavior has been tested in Figure 6 and although the fit is good the parameters are not realistic enough (see above). Nonetheless it is possible to modify the previous formula in order to work in the neighborhood of the phase transition

$$t_n = t(l_n) \sim \tau_0 l_n^{z_c} \exp \left(\frac{\Upsilon(T) l_n^\psi}{k_B T} \right), \quad (26)$$

with $\Upsilon(T) = \Upsilon_0(T_c - T)^{\nu\psi}$. Near the phase transition this formula reduces to the usual (non activated) formula $\tau \simeq l_n^{z_c}$.

To test this generalization of the original droplet formula it is interesting to compute experimentally the following function (using the same procedure as in ref. [61]):

$$G(t_w, T) = \left(\frac{\log(t_w/\tau_0) - \frac{z_c}{3} \log N_s(t_w, T)}{\frac{T_g}{T} N_s(t_w, T)^{\psi/3}} \right)^{\frac{1}{\nu\psi}}. \quad (27)$$

In Figure 7, $G(t_w, T)$ is shown against T/T_g for different waiting times, temperatures and three different spin glasses with different critical temperatures. The linear fit, supporting equation (26), is very good and the points extrapolate to near 1 when G approaches zero.

In addition, Berthier and Bouchaud, in ref. [60], have tested this scenario via numerical simulations. In particular in four dimensions they have found that this droplet generalization works well. However the microscopic time they obtained in their fits shows (in three dimensions) a non monotonic dependence on the temperature, for which there is not physical explanation [60].

⁷We introduce in this discussion the Boltzmann constant, k_B , which has been set to one in the rest of the paper.

⁸By inverting in this formula l_n in terms of t_n we obtain the activated dynamics prediction for the dynamical correlation length, see equation (23).

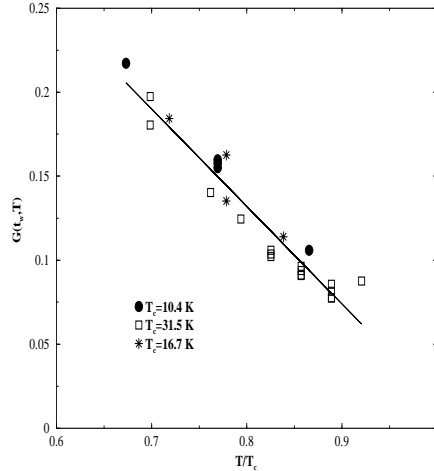


Figure 7: Plot of $G(t_w, T)$, defined in the text, against T/T_g for different waiting times, temperatures and three spin glasses with different critical temperatures T_g . The authors have used $\psi = 1.5$, $\nu = 1.3$ and $z_c = 5$ motivated by the experimental study of AgMn. If $z_c = 6$ is assumed then the data extrapolate to $T/T_g = 1$. The scaling is very good. From reference [62].

4 Off equilibrium fluctuation-dissipation relations

One of the most important results of Statistical Physics at equilibrium is the so-called fluctuation-dissipation theorem. In this section we will review its theoretical basis and its generalization at early times in the dynamics. Moreover we will see how this generalization provides us with a useful tool to understand which are the properties of the low temperature phase at equilibrium.

4.1 Theoretical basis

The starting point is to perturb the original Hamiltonian, \mathcal{H} , of a spin glass in a magnetic field as

$$\mathcal{H}' = \mathcal{H} + \int \Delta h(t) A(t) dt , \quad (28)$$

where

$$\mathcal{H} = - \sum_{\langle i,j \rangle} J_{ij} \sigma_i \sigma_j + h \sum_i \sigma_i , \quad (29)$$

h being the magnetic field. We can define the following autocorrelation function

$$C(t_1, t_2) \equiv \langle A(t_1) A(t_2) \rangle . \quad (30)$$

Usually, $A(t) = \sigma_i(t)$, and the associated response function

$$R(t_1, t_2) \equiv \left. \frac{\delta \langle A(t_1) \rangle}{\delta \Delta h(t_2)} \right|_{\Delta h=0}. \quad (31)$$

The brackets $\langle \dots \rangle$ in eq. (30) and eq. (31) imply here a double average, one over the dynamical process and one over the disorder.

In the dynamical framework, assuming time translational invariance, it is possible to derive the fluctuation-dissipation theorem (FDT), that reads

$$R(t_1, t_2) = \beta \theta(t_1 - t_2) \frac{\partial C(t_1, t_2)}{\partial t_2}, \quad (32)$$

where $\beta = 1/T$ is the inverse temperature.

The fluctuation-dissipation theorem holds in the equilibrium regime, but in the early times of the dynamics one expects a breakdown of its validity. Mean Field studies [65, 66, 67] suggest the following modification of the FDT (OFDR hereafter):

$$R(t_1, t_2) = \beta X(C(t_1, t_2)) \theta(t_1 - t_2) \frac{\partial C(t_1, t_2)}{\partial t_2}. \quad (33)$$

where X defines the violation of fluctuation-dissipation. We can use the previous formula, eq. (33), to relate the observable quantities defined in eq. (30) and eq. (31). In the linear response regime, the magnetization can be written as (we report for completeness the formulas obtained for a Ising spin glass in a magnetic field, so $m[h](t) \neq 0$)

$$\begin{aligned} m[h + \Delta h](t) &= m[h](t) \\ &+ \int_{-\infty}^t dt' \left. \frac{\delta m[h'](t)}{\delta h'(t')} \right|_{h'(t)=h(t)} \Delta h(t') + \mathcal{O}(\Delta h^2) \end{aligned} \quad (34)$$

and so,

$$\Delta m[h, \Delta h](t) = \int_{-\infty}^t dt' R(t, t') \Delta h(t') + \mathcal{O}(\Delta h^2), \quad (35)$$

where we have defined $\Delta m[h, \Delta h](t) \equiv m[h + \Delta h](t) - m[h](t)$. Eq. (35) is just the linear-response theorem neglecting higher orders in Δh . By applying the OFDR we obtain the dependence of the magnetization with time in a generic time-dependent magnetic field (with a small strength), $\Delta h(t)$,

$$\Delta m[h, \Delta h](t) \simeq \beta \int_{-\infty}^t dt' X[C(t, t')] \frac{\partial C(t, t')}{\partial t'} \Delta h(t'). \quad (36)$$

Next we let the system evolve with the unperturbed Hamiltonian until $t = t_w$ and then we turn on the perturbing magnetic field Δh (hence, the system feels a magnetic field $h + \Delta h$)⁹. Finally, with this choice of the magnetic field, we can write

$$\Delta m[h, \Delta h](t) \simeq \Delta h \beta \int_{t_w}^t dt' X[C(t, t')] \frac{\partial C(t, t')}{\partial t'} \quad (37)$$

and

$$\Delta m[h, \Delta h](t) \simeq \Delta h \beta \int_{C(t, t_w)}^1 du X[u] , \quad (38)$$

where we have used the fact that we are working with Ising spins. In the equilibrium regime ($X = 1$, as the fluctuation-dissipation theorem holds) we must obtain

$$\Delta m[h, \Delta h](t) \simeq \Delta h \beta (1 - C(t, t_w)) , \quad (39)$$

i.e., $\Delta m[h, \Delta h](t) T / \Delta h$ is a linear function of $C(t, t_w)$ with slope -1 .

In the limit $t, t_w \rightarrow \infty$ with $C(t, t_w) = q$, one has that $X(C) \rightarrow x(q)$, where $x(q)$ is given by

$$x(q) = \int_{q_{\min}}^q dq' P(q') , \quad (40)$$

where $P(q)$ is the equilibrium probability distribution of the overlap with support $[q_{\min}, q_{\max}]$. Obviously $x(q)$ is equal to 1 for all $q > q_{\max}$, and we recover FDT for $C(t, t_w) > q_{\max}$. This link between the dynamical function $X(C)$ and the static one $x(q)$ has been already verified for finite dimensional spin glasses [68]. The link has been analytically proved for systems with the property of stochastic stability [70].

We remark that we can use this formula to obtain q_{\max} as the point where the curve $\Delta m[h, \Delta h](t)$ against $C(t, t_w)$ leaves the line with slope $-\beta \Delta h$.

For further use, we define

$$S(C) \equiv \int_C^1 dq x(q) , \quad (41)$$

or equivalently

$$P(q) = - \left. \frac{d^2 S(C)}{d^2 C} \right|_{C=q} . \quad (42)$$

In the limit where $X \rightarrow x$ we can write eq. (38) as

$$\frac{\Delta m[\Delta h](t) T}{\Delta h} \simeq S(C(t, t_w)) . \quad (43)$$

⁹In the first numerical application of this method, Franz and Rieger [69] chose another dependence of the magnetic field with time: $h(t) = h_0 \theta(t_w - t)$.

Looking at the relation between the correlation function and the integrated response function for large t_w we can thus obtain q_{\max} , the maximum overlap with non-zero probability, as the point where the function $S(C)$ becomes different from the function $1 - C$.

From the function $S(C)$ we can get information on the overlap distribution function $P(q)$, through eq. (42). Let us recall which is the prediction for the $S(C)$ assuming the validity of each one of the competing theories described in the introduction. The droplet model predicts $P(q) = \delta(q - \hat{q})$ and consequently¹⁰

$$S(C) = \begin{cases} 1 - \hat{q} & \text{for } C \leq \hat{q}, \\ 1 - C & \text{for } C > \hat{q}. \end{cases} \quad (44)$$

On the other hand the RSB prediction for the overlap distribution[6], $P(q) = (1 - x_M)\delta(q - q_{\max}) + x_M\delta(q - q_{\min}) + \tilde{p}(q)$ (where the support of $\tilde{p}(q)$ belongs to the interval $[q_{\min}, q_{\max}]$, $q_{\min} \propto h^{4/3}$ and q_{\max} mainly depends on the temperature), implies that

$$S(C) = \begin{cases} S(0) & \text{for } C \leq q_{\min}, \\ \tilde{s}(C) & \text{for } q_{\min} < C \leq q_{\max}, \\ 1 - C & \text{for } C > q_{\max}, \end{cases} \quad (45)$$

where $\tilde{s}(C)$ is a quite smooth and monotonically decreasing function such that

$$\tilde{p}(q) = - \left. \frac{d^2 \tilde{s}(C)}{dC^2} \right|_{C=q}. \quad (46)$$

In Figure 8 we show three possible behaviors of the function $S(C)$ (and for the closely related function $P(q)$).

To finish this section we will recall an approximate scaling property of the probability distribution of the overlap that was introduced by Parisi and Toulouse (hereafter PaT) [71]. In particular in Mean field the PaT hypothesis implies¹¹

$$S(C) = \begin{cases} 1 - C & \text{for } C \geq q_{\max}, \\ T\sqrt{1 - C} & \text{for } q_{\min} \leq C \leq q_{\max}. \end{cases} \quad (47)$$

¹⁰In models with only one state, as the droplet model predicts for the Ising spin glass in a magnetic field, the equilibrium time is finite irrespective of the value of the volume of the system, hence, we can always thermalize any volume, and so the asymptotic behavior, for waiting times larger than the equilibration time, consists only of the straight line $1 - C$. There is no horizontal part.

¹¹The goodness of this approximate Ansatz has been studied in reference [72] in the Mean Field approximation. They find that none of the Parisi-Toulouse scaling hypotheses about the $q(x)$ behavior hold, but some of them are only violated at higher orders (taking as the parameter of the expansion the reduced temperature).

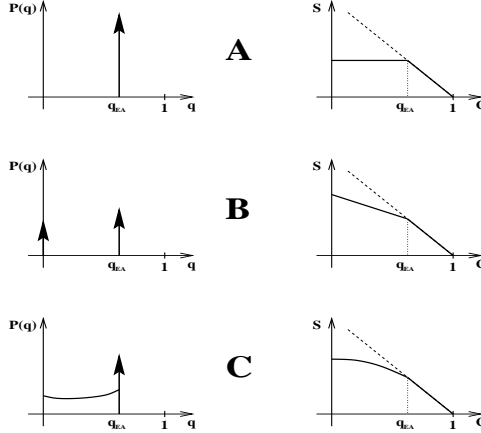


Figure 8: A possible model classification based on the function $S(C)$. The big arrows represent delta functions. (A) corresponds to droplet model, (B) to one step of replica symmetry breaking and (C) to continuously broken replica symmetry (e.g., Parisi solution of an infinite dimensional Ising spin glass in absence of magnetic field). Taken from reference [80].

The result for $C \geq q_{\max}$ is general (and true for finite dimension) and for $q_{\min} \leq C \leq q_{\max}$ we make the following Ansatz: $S(C) = AT(1-C)^B$ (in RSB $A = 1$ and $B = 1/2$). If we substitute this Ansatz in eq. (43) we obtain the following scaling equation

$$\frac{mT}{h} T^{-\phi} = f \left((1-C) T^{-\phi} \right), \quad (48)$$

where f is a scaling function and $\phi = 1/(1-B)$ (in Mean Field $\phi = 2$). In order to be consistent, the scaling function should be composed by a linear part (x) and by a power law part (Ax^B).

In the rest of this section, we will discuss numerical simulations and experiments.

4.2 Numerical Results

In Figure 9 we show the numerical points obtained for two very large waiting times (in order to control that no dependence on t_w is found) and the prediction from the statics: $x(q)$. As a control we have computed the final point of the curve (the $C = 0$ point) extrapolating at infinite time the magnetization using a power law fit. The agreement is very good. Notice that the asymptotic curve, which we can identify

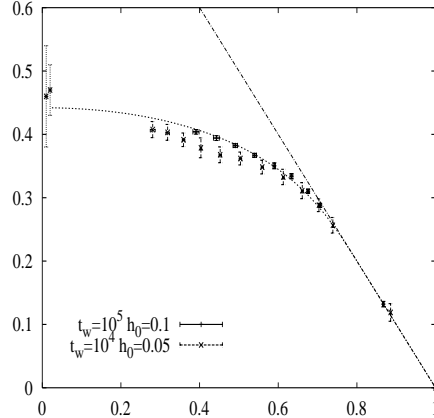


Figure 9: Off equilibrium fluctuation-dissipation relation. We plot $m(t, t_w)T/h$ versus the spin-spin correlation function $C(t, t_w)$ at $T \simeq 0.7T_c$. The lattice simulated was $L = 64$ and we show two waiting times and two perturbing magnetic fields in order to control that linear response holds. The straight line with -1 slope is the equilibrium prediction. All the points on this line are pseudo-equilibrium points. We have marked the extrapolation to infinite time of the susceptibility with the two leftmost points in the plot. Finally we have computed the $x(q)$ function at equilibrium (from the numerical simulation, using parallel tempering [76, 77], of a $L = 16$ lattice). Taken from reference [68].

with the largest waiting time in the figure, is not compatible with the prediction for the droplet model (a horizontal part followed by the pseudo-equilibrium one) [68].

From this figure, we can compute the Edwards-Anderson order parameter ($q_{\text{EA}} = q_{\max}$) as the point at which the numerical points depart from the pseudo-equilibrium region (the straight line $1 - C$). We can estimate $q_{\text{EA}} \simeq 0.7$. If the droplet model holds the order parameter should be $q_{\text{EA}} \simeq 0.55$ (in the DM, the asymptotic curve should be a horizontal straight line in the region $[0, q_{\text{EA}}]$; the final point $C = 0$ is provided by the infinite time extrapolation of the susceptibility, we can compute $q_{\text{EA}} = 1 - mT/h|_{\text{asyn}}$).

We can test these possible values for q_{EA} . To do this we recall equilibrium numerical simulation performed using parallel tempering [76, 77] in a wide range of lattice sizes: $L = 4, 6, 8, 10$ and 16 . We plot in Figure 10 the equilibrium probability distribution of the overlap $P(q)$. We can define $q_{\text{EA}}(L)$ as the value of q in which $P(q, L)$ shows a maximum. Furthermore we can analyze the dependence

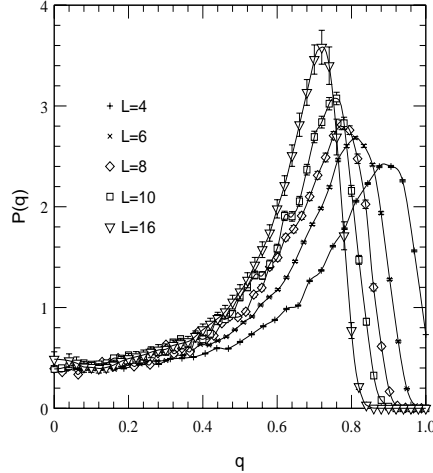


Figure 10: Overlap probability distribution for $L = 4, 6, 8, 10$ and 16 at $T \simeq 0.7T_c$. Taken from [57, 75].

of $q_{\text{EA}}(L)$ with L . The simplest dependence is a power law:

$$q_{\text{EA}}(L) = q_{\text{EA}}^\infty + \frac{a}{L^b}, \quad (49)$$

where a and b are constants. In Figure 11, we show $q_{\text{EA}}(L)$ versus $L^{-1.5}$ together with a linear fit [75]. Therefore, the data can be described with great accuracy assuming a power law with a non zero value of $q_{\text{EA}}^\infty \simeq 0.7$. Finally, the data does not support a power law fit with final value $\simeq 0.55$.¹² Therefore we have obtained two compatible estimates of q_{EA} at $T = 0.7$ using an off-equilibrium technique and an equilibrium one and both results agree in the statistical error.

This technique can be implemented in experiments. This has been done in reference [73] by studying the $\text{CdCr}_{1.7}\text{In}_{0.3}\text{S}_4$ insulating spin glass with $T_g = 16.2\text{K}$. One measures the response and the autocorrelation between the spins. The first part of the work is not difficult, but the latter one has posed a challenge to the experimentalists. We report in Figure 12 the plot of the violation of FDT. In contrast with what happens in numerical simulations (where there is not a measurable dependence of the curves with the waiting time for the larger times simulated. See Figures 3 and 4 of reference [35] for a detailed study of the L and t_w dependences),

¹²Incidentally, in the droplet model the probability of having an overlap different from the maximum one (q_{EA}) goes to zero as $L^{-\theta}$. It is clear that data in Figure 10 rule out this possibility. In particular, $P(0) \rightarrow \text{const} \neq 0$. The same conclusion is reached if one works with window overlaps instead of the total ones [81].

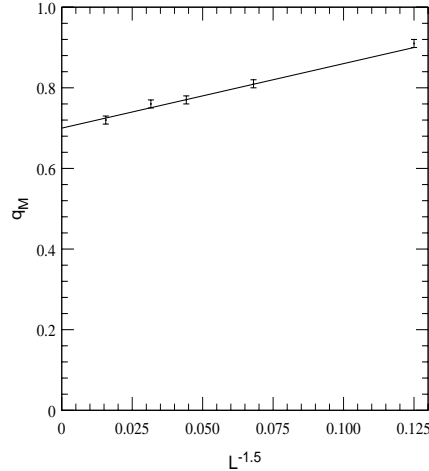


Figure 11: Value of the overlap in which the probability distribution shows a maximum as a function of the lattice size at $T \simeq 0.7T_c$. From [75].

in the experiment a strong dependence has been found for the reported curves with the waiting time, thus, an extrapolation to large (infinite) waiting time is mandatory. This extrapolation is the dashed line shown in the figure. Notice also the dot-dashed line in Figure 12 which corresponds to the quasi-equilibrium regime. If one believes the extrapolation, the figure supports heavily the RSB scenario and discards that of the droplet model.

Finally, we will end this section by showing a scaling analysis of the off-equilibrium fluctuation-dissipation relations. This has been done by using the PaT scaling which applies with great precision to the equilibrium probability distribution, although it is not exact. In Figure 13 we report the scaling plot and it can be seen that is a really good scaling (different magnetic fields, in order to control linear response, waiting times, to check asymptoticity, and temperatures) [74].

Notice that the PaT scaling works for L and t_w independent curves (see Figure 9 and reference [35]). Two clear and distinctive regimes can be seen in that figure. The first one correspond to the quasi-equilibrium regime: in that part of the figure the behavior is linear and thus it matches with the quasi-equilibrium regime $\Delta mT/h = 1 - C$. The second one corresponds to the aging regime: that part of the plot can be parametrized with a power law with the B exponent introduced above.¹³

¹³Following reference [78] this kind of scaling is not enough to detect a RSB phase (they found in the two dimensional Ising model—with no phase transition at finite temperature—a PaT scaling for their OFDR). Nevertheless, in [78] the PaT scaling only works for points with the same waiting

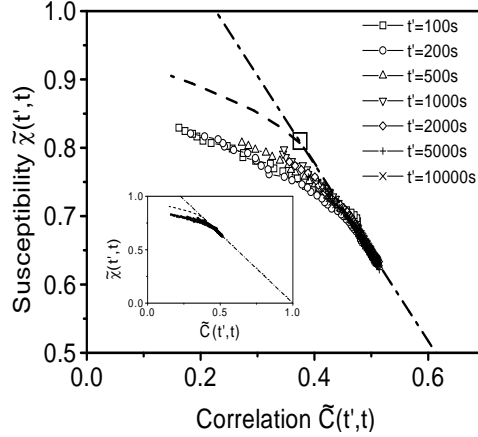


Figure 12: Experimental determination of the function X which induces the violation of fluctuation-dissipation. See the text for more details. Taken from reference [73].

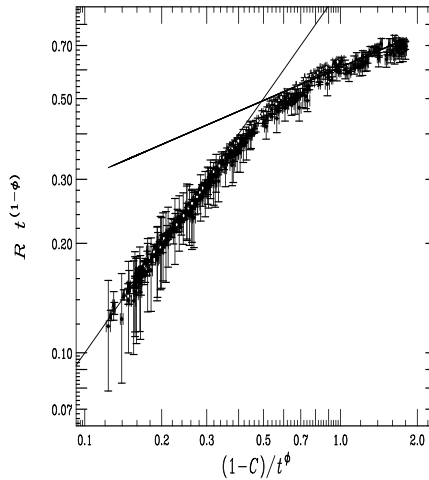


Figure 13: PaT scaling for the three dimensional Ising spin glass ($h = 0$). The plot has been built with L and t_w independent curves in order to check that we are in the asymptotic regime. Taken from reference [74].

5 Memory and rejuvenation

Maybe the most striking features of spin glasses were found in experiments where cycles in temperature were done. We are referring to the so-called memory and rejuvenation effects.

In Figure 14 we show an experimental plot reported in Ref. [63]. In this experiment, a sudden quench from high temperature is done to a temperature ($T = 12\text{K}$) below the critical one ($T_g = 16.2\text{ K}$). At this point the out of phase susceptibility is recorded. At a certain point of the experiment the temperature is lowered again (in this case to $T = 10\text{ K}$) and the out of phase susceptibility is recorded again. As can be seen in Figure 14 the out of phase susceptibility, measured at the new temperature (10 K), starts from a higher value than the susceptibility that the system had just before the quench from 12K to 10K. This is known as the rejuvenation of the system. When we cold a system it behaves as if it was younger than before, *i.e.*, its out-of phase susceptibility is higher than the one the system had at the higher temperature just before the quench. In plain words, the system at the new, lower temperature is farther from equilibrium than in the last moments at the higher temperature. One can stay at the lower temperature for a while and then restore the temperature of the system to the original one (*i.e.*, we heat the system from 10 K to 12 K). In Figure 14 we see that the system recovers the value of the out of phase susceptibility that it had just before it was cooled to 10 K. This phenomenon is known as memory effect. Notice in the inset of Figure 14 how, despite the strong relaxation produced at 10 K, the curves obtained in the higher temperature $T = 12\text{ K}$ in two separated time intervals are in smooth continuation. In reference [64] the reader can see good, recent and detailed experimental studies of rejuvenation and memory effects.

Berthier and Bouchaud [60] have recently obtained rejuvenation and memory in the four dimensional Ising spin glass. We reproduce in Figure 15 their results. In three dimensions they have not seen these effects [60].

As a numerical approximation to the ac out of phase susceptibility Berthier and Bouchaud [60] proposed to use:

$$\chi(\omega, t_w) = \frac{1}{T} \left(1 - C(t_w + \frac{1}{\omega}, t_w) \right), \quad (50)$$

where $C(t, t')$ is the spin-spin dynamical correlation defined in eq. (30).

time, instead, in the plot we have points computed with different waiting times. In effect, we remark again, the scaling reported in Figure 13 is t_w -independent (at least in the numerical precision) which is a behavior completely different from the two dimensional spin glass (paramagnetic phase). For a paramagnetic phase and very long waiting time (*i.e.* all the points lie in the $1 - C$ straight line) the PaT scaling plot should consist in points over the linear part (quasi-equilibrium regime), and none in the power law part (aging regime).

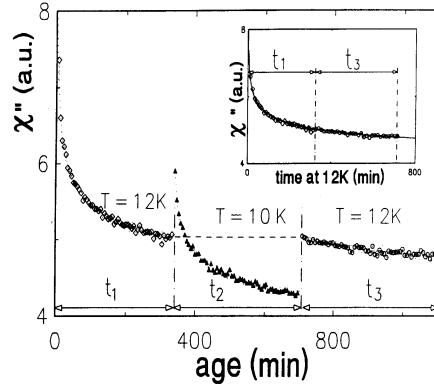


Figure 14: Rejuvenation and memory in a real Ising spin glass. Out of phase susceptibility, $\chi''(\omega, t_a)$, of $\text{CdCr}_{1.7}\text{In}_{0.3}\text{S}_4$, with critical temperature $T_g = 16.2\text{K}$, during a cycle in temperature. The frequency, ω , is 0.01 Hz and t_a is the time elapsed since the quench. The figure inset shows that, despite the strong relaxation at 10 K, both part at 12 K are in perfect continuation of each other. From [63].

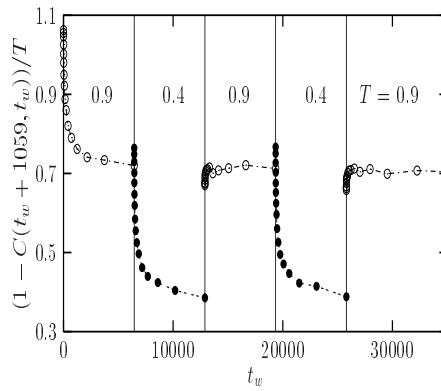


Figure 15: Rejuvenation and memory in the numerical simulation of the four dimensional Ising spin glass. Evolution of the ac correlation function following the schedule: $T = \infty \rightarrow T_1 = 0.9 \rightarrow T_2 = 0.4 \rightarrow T_1 \rightarrow T_2 \rightarrow T_1$. Notice that the critical temperature for this model is $T_c = 1.8$. Taken from [60].

Following Berthier and Bouchaud we can try to explain memory and rejuvenation effects in terms of the dynamical correlation length [60].

Let us first consider rejuvenation. The system at the higher temperature (T_1) thermalizes its so-called fast modes (*i.e.*, $\xi(t, T_1) \ll L$). When the system is frozen to a low temperature, these fast modes that are just equilibrated at the higher temperature are out of equilibrium in the new one, and so the system at the new lower temperature, is younger than before ($\xi(t_1, T_2) \ll \xi(t_1, T_1)$, where t_1 is the time the system elapses in $T = T_1$). This mechanism does not rely on the concept of chaos in spin glasses [64]¹⁴.

The memory effect can be understood as follows. We have said that rejuvenation involves the reorganization of small scales as compared to the lengths involved in the aging at T_1 , the higher temperature. When we heat the system from T_2 to T_1 , these small scales “almost instantaneously” equilibrate at T_1 , and the aging restarts at T_1 at the same point. More quantitatively: the time needed for the system to recover its age at T_1 is given by $\xi(t_{\text{memory}}, T_1) \simeq \xi(t_2, T_2)$, where t_2 is the time elapsed in T_2 . If $T_1 - T_2$ is “large” then $t_{\text{memory}} \ll t_2$. So, in this interpretation, memory is based in the existence of two, well separated, scales, while rejuvenation is based in the reorganization of small scales.

6 Spin glass at zero temperature

In the last years a large amount of numerical work has been devoted to numerical simulations at zero temperature. In particular has been studied the influence of perturbations in the ground state of the system. We will study in the next two subsections, two way to perturb the system and we will discuss the results in the light of the three scenarios (RSB, DM and TNT).

6.1 Changing the boundary conditions

We will review in this section numerical simulations performed at zero temperature in which ground states of the system are computed with great accuracy.

¹⁴Chaos, in this context, refers to the sensitivity of equilibrium states in the ordered phase to small changes in the couplings or in temperature. Temperature chaos postulates that typical equilibrium configuration at two different temperatures T_1 and T_2 respectively, are strongly correlated in a distance l_0 which depends on $\Delta T = T_1 - T_2$. For distances larger than l_0 the correlations between these two typical configuration go to zero. Scaling arguments provides $l_0 \sim |\Delta T|^{1/a}$, where $a = d_s/2 - \theta$, d_s is the fractal dimension of the interface (see next section) and θ is the usual droplet exponent. The change of the equilibrium states as we change temperature explains rejuvenation. In Mean Field the effect of chaos in temperature is minimal [26]. In numerical simulations no clear chaos effects have been detected [27], but see [28]; for a droplet interpretation, see [29].

One interesting observable is the link overlap (we will study in the next section its properties at finite temperature) defined by [79]:

$$q_l(i, \mu) = q(i)q(i + \mu) \quad (51)$$

where $q(i) = \sigma(i)\tau(i)$ is the overlap, where σ/τ belong to a ground state that has been computed using periodic/antiperiodic boundary conditions respectively, and by μ we are denoting one of the d unitary vectors that can be defined in a d -dimensional hypercubic lattice (and so $i + \mu$ is the point of the lattice neighbor of i in the direction provided by the vector μ).

Neglecting the points at the boundary, we can define the interface between both ground state configurations as the region of space in which $q_l(i, \mu) = -1$. The probability to pick up such interface on a given random link, l , is given by

$$\rho = \frac{1}{2}(1 - \overline{q_l}) , \quad (52)$$

where by $\overline{q_l}$ we denote the disorder expectation of $q_l(i, \mu)$ averaged over all sites, i , and directions, μ .

At this point one is faced with three possibilities (there are an additional fourth, but, we refer to the reader to reference [79] for a detailed explanation):

1. The interface is confined to a region of width L^z , with $z < 1$; inside of this region the interface could have overhangs. In this case ρ goes to zero following a pure power law $L^{-\alpha}$, where $\alpha \geq 1 - z$.¹⁵
2. The wandering exponent z is equal to 1 and the interface is a fractal object (not a multifractal) with fractal dimension, d_s . Then $\rho \sim L^{-\alpha}$ with $\alpha = d - d_s$.
3. The exponent α is zero and the probability, ρ , goes to constant. Hence the interface is space filling. This last possibility is realized in the RSB scenario.

Let us consider some examples. In a ferromagnet the ground state obtained with antiperiodic boundary conditions (a.b.c.) should be locally similar to that obtained with periodic boundary conditions (p.b.c.), modulo an interface. As the interface, which is a flat surface, has no measure, the link overlap between these two ground states should be 1 in the large volume limit. In the droplet picture of spin-glasses the discussion is similar. The only difference with the previous example is that the interface is not necessarily flat rather it could be a corrugated

¹⁵Roughly, the volume of the interface is $L^{d-1} \times L^z$. To obtain the probability we must divide the interface volume by the space volume, obtaining the relation between α and z .

surface (scenario 2). On the other hand, the RSB of spin-glasses is different: The ground state obtained under a.p.b. is expected to be locally similar to one of the low energy states of the spectrum of the p.b.c. case. Thus, the link overlap between these two ground states should tend in the large volume limit to a constant value different from 1.

By computing ground states, Marinari and Parisi reported the following values for the link overlap computed using four different methods [79]: $q_l = 0.755(15)$, $0.80(6)$, $0.732(8)$ and $0.722(5)$ (these figures have been extrapolated to $L \rightarrow \infty$). Putting all four results together, we can finally quote

$$q_l = 0.79(7). \quad (53)$$

Note that q_l is three standard deviations away from the droplet prediction $q_l = 1$.

We can try to recover this figure by performing numerical simulations at finite temperature and then try to extrapolate the data to zero temperature. This has been done in reference [82] by noting that since the overlap between the ground state computed with two different boundary conditions (since the change of boundary conditions can be regarded as a strong perturbation and the corresponding ground states are far away) is expected to be very small we can use the dynamical numerical simulations reported in the previous section (in which the overlap remains almost zero all the run) in order to obtain the value of the link overlap. It is easy to obtain q_l since it is nothing but $C_{\text{eq}}(x = 1)$ (see eq. (19)). In Figure 16 we plot the values of $C_{\text{eq}}(1)$ obtained for different temperatures and we also mark the value obtained at zero temperature, see eq. (53). The consistency of both sets of data is very good. We will come back to this issue at the end of this section.

6.2 Bulk perturbations

Another way to perturb the system is to add a perturbation to the couplings of the model [4, 87]. The new Hamiltonian reads:

$$\mathcal{H}' = \mathcal{H} + \frac{\epsilon}{N_B} \sum_{\langle i,j \rangle} \sigma_i^0 \sigma_j^0 \sigma_i \sigma_j, \quad (54)$$

where $N_B = dL^d$ is the number of bonds, ϵ is the strength of the perturbation and $\{\sigma^0\}$ is the ground state configuration computed with no perturbation (e.g., $\epsilon = 0$). The sum $\sum_{\langle i,j \rangle}$ is extended over all pairs of nearest neighbors.

We can define the following link overlap

$$q_l^{(\alpha,0)} = \frac{1}{N_B} \sum_{\langle i,j \rangle} \sigma_i^0 \sigma_j^0 \sigma_i^\alpha \sigma_j^\alpha. \quad (55)$$

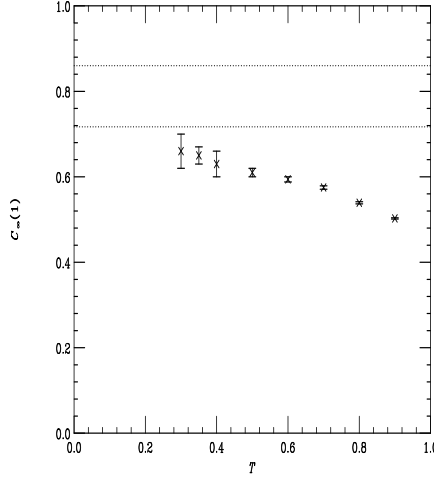


Figure 16: Values extrapolated to infinite time of the correlation function at distance $x = 1$, $C_\infty(1, T) \equiv C_{\text{eq}}(x = 1, T)$, versus T . We have also marked by two horizontal dotted lines the interval where the value computed in reference [79] lies, using $T = 0$ ground state calculations. The consistency of the two results is clear.

One overlap can be defined in the usual way

$$q = \frac{1}{L^d} \sum_i \sigma_i^0 \sigma_i^\alpha . \quad (56)$$

Hence, we can write eq.(54) as

$$\mathcal{H}' = \mathcal{H} + \epsilon q_l^{(\alpha,0)} , \quad (57)$$

where we have labeled the configuration $\{\sigma\}$ by the index α .

One can show that the original ground state energy is shifted by an amount ϵ (since $q^{(0,0)} = 1$); the energy of any other state α (e.g., a low lying excitation of the spectrum) is shifted by an amount $\epsilon q_l^{(\alpha,0)}$.

Let ΔE be the gap between the α state and the ground state one in absence of perturbation. If $\epsilon > \epsilon q_l + \Delta E$ the new ground state should be the α one.

One can compute the droplet prediction for the probability of this event. In the

DM the probability to have an excitation of energy E is given by¹⁶

$$P(E) = \frac{1}{L^{\theta'}} f\left(\frac{E}{L^{\theta'}}\right), \quad (58)$$

and so the probability to have an excitation with energy less than $\epsilon(1 - q_l)$ is given by

$$P_< = \int_0^{\epsilon(1-q_l)} dE P(E) = g\left(\frac{\epsilon}{L^\mu}\right), \quad (59)$$

where we have used that $1 - q_l \simeq L^{-(d-d_s)}$ and $g(u) \equiv \int_0^u ds f(s)$ ¹⁷. Finally $\mu = \theta' + d - d_s$. Now we can write the following scaling function for the overlap and the link overlap (which are given by the product of the probability of having a favorable droplet $P_<$, times the contribution of this droplet to $1 - \bar{q}$ and $1 - \bar{q}_l$ respectively, see the previous footnote)

$$1 - \bar{q} \propto g\left(\frac{\epsilon}{L^\mu}\right), \quad (60)$$

$$1 - \bar{q}_l \propto \frac{1}{L^{(d-d_s)}} g\left(\frac{\epsilon}{L^\mu}\right). \quad (61)$$

We remark that by \bar{q} and \bar{q}_l we denote the average of the overlap and the link overlap over the disorder, respectively. For small ϵ , assuming $f(0) \neq 0$, we obtain the following asymptotic formulas

$$1 - \bar{q} \sim \frac{1}{L^{d-d_s+\theta'}}, \quad (62)$$

$$1 - \bar{q}_l \sim \frac{1}{L^{2(d-d_s)+\theta'}}. \quad (63)$$

Palassini and Young found for the three dimensional Gaussian spin glass with periodic boundary conditions [4]

$$\theta' = 0.02(3), \quad d - d_s = 0.42(2), \quad \mu = 0.42(3), \quad (64)$$

and in four dimensions [4]

$$\theta' = 0.03(5), \quad d - d_s = 0.23(2). \quad (65)$$

¹⁶It has been assumed that the probability of an excitation on the ground state scales as $L^{\theta'}$. In the droplet picture the θ exponent is defined computing the scaling of the difference of free energies from boundary condition changes. It turns out that the droplet picture predicts $\theta = \theta'$.

¹⁷In the droplet picture there are only two thermodynamic states related by spin-flip reversal symmetry. The overlap between a droplet and the ground state is one minus a term which scales as the volume of the droplet (L^d) divided by the volume of the system (L^d). The link overlap in this circumstance differs from 1 by a factor which is the volume of the interface of the droplet (L^{d_s}) over the total volume (L^d). We are assuming that the excitation is one droplet with size proportional of that of the lattice size [4].

This implies a non trivial probability distribution for the overlap but a trivial one for the link overlap.

However the RSB scenario cannot be ruled out by the data because it is possible to fit $1 - \bar{q}_l$ and $1 - \bar{q}_l$ to a constant plus scaling corrections, *i.e.*,

$$1 - \bar{q}_l = a + \frac{b}{L^c} \quad (66)$$

with $a = 0.28(3)$ (*i.e.*, $q_l = 0.72(3)$), b and c being positive constants. Indeed, these are scaling-corrections that are compatible with the RSB prediction: $\theta' = 0$ and $d = d_s$.

On the other hand, the droplets prediction is $\theta' = \theta \simeq 0.2$ (in three dimensions) and $d - d_s > 0$.

Krzalaka and Martin reached the same conclusions [3]. Next, Houdayer, Krzakala and Martin [84] studied the topological properties of these excitations finding sponge-like conformations (this provides a geometrical picture [83] for the RSB scenario) which costs $\mathcal{O}(1)$ in energy; finally they concluded that large finite size effects should be presented in order to explain the data with the RSB picture¹⁸. Related work by this group can be found in references [85].

Therefore they propose [3, 4], assuming the absence of strong scaling corrections, an intermediate or mixed scenario between droplet and RSB, the so called TNT picture (TNT for trivial (q_l), non trivial (q)).

Yet, the controversy is not settled. In reference [87] Marinari and Parisi analyzing the data assuming RSB obtained

$$1 - q_l(q = 0) = 0.245(15) \quad (67)$$

and by the study the correlation functions $1 - q_l(q = 0) = 0.33(2)$. Here $q_l(q = 0)$ denotes that the link overlap has been computed using only configurations with mutual zero overlap. Moreover it has been found that $q_l(q)$ depends quadratically on q , as found in infinite dimension.

In addition, reference [86] has obtained, by simulating the three dimensional Gaussian Ising spin glass *but* with free boundary conditions (in this reference the ground states were computed in an exact way)

$$1 - \bar{q}_l^c = 0.20(2) , \quad (68)$$

where the superscript c denotes the average over those samples in which the unperturbed and perturbed ground states are very different (*i.e.*, the overlap is less than a

¹⁸Houdayer, Krzakala and Martin provide three values for the link overlap in their paper: $q_l = 0.68, 9.72$ and 0.75 depending on the number of parameters used in their fits.

given threshold value, $q_{\max} = 0.4$. Another cutoff $q_{\max} = 0.2$ gives essentially the same results). This value is in very good agreement with that obtained by Marinari and Parisi and cited above in this section (see eqs. (53) and (67)). However, the authors also found that if scaling corrections are allowed into the droplet prediction, then an equally good fit is found, and one obtains

$$\theta' = 0.19(6) , \quad d - d_s = 0.44(3) , \quad \mu = 0.63 . \quad (69)$$

Notice that $\theta' = \theta \simeq 0.2$ as the droplet picture predicts, but in contradiction with TNT.¹⁹

7 (More on) The link overlap (at finite temperature)

The aim of this section is to study the properties of the link-overlap q_l *but* at finite temperature [88, 89]. The goal here is to characterize the probability distribution of the overlap computing its variance. It has been found that

$$\text{var}(q_l) \sim L^{-\mu_l} . \quad (70)$$

It is possible to compute the μ_l exponent as a function of θ' and d_s , the fractal dimension of an excitation. If we assume that this variance is dominated by the contribution of a single droplet of size L , then this event occurs with probability $T/L^{\theta'}$ (assuming a constant density of states for these excitations, *i.e.*, $f(0) \neq 0$, see eq. (58)). We have seen that $1 - q_l$ is proportional to $L^{-(d - d_s)}$. The same holds true for δq_l . Hence, the variance (which is the mean value of δq_l^2) is given by

$$\text{var}(q_l) \sim \frac{T}{L^{\theta'}} L^{-2(d - d_s)} , \quad (71)$$

and so $\mu_l = \theta' + 2(d - d_s)$. The link overlap probability distribution obtained with numerical simulation of the three dimensional Ising spin glass with periodic boundary conditions is shown in Figure 17. In the droplet model this probability distribution should shrink to a Dirac delta (zero variance); instead, in RSB $P(q_l)$ should have a compact support (and so non zero variance).

The extrapolation of the μ_l exponent to zero temperature gives a value: $\mu_l = 0.76(3)$. By assuming $\theta' = 0$ this implies that $d - d_s = 0.38(2)$, near the value computed directly at $T = 0$ using ground state computations: $d - d_s = 0.42(2)$ (see preceding section). However, a fit assuming RSB (*i.e.*, $\mu' = 0$) cannot be ruled out by the numerical data [88].

¹⁹Incidentally, the relation between the link overlap and the overlap has been study in this reference [86] obtainig $q_l = 0.77(2) + 0.27(3)q^2$, according with RSB predictions. Moreover $q_l(q = 0) = 0.77(2)$.

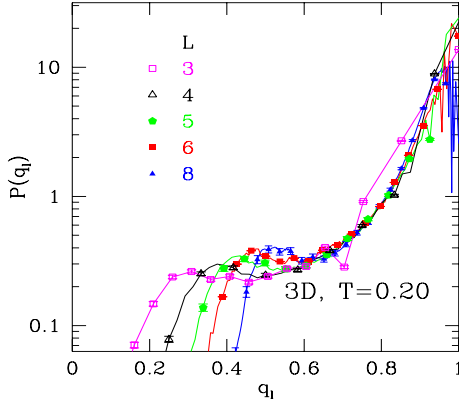


Figure 17: $P(q_l)$ for the three dimensional Gaussian spin glass at $T = 0.2$ for different lattice sizes with periodic boundary conditions. Taken from reference [88].

In reference [89] free boundary conditions (f.b.c) were used. With this f.b.c they try to discern between a trivial behavior for the link overlap given by $\text{var}(q_l) \sim L^{-e}$ with a suitable e exponent, and the RSB behavior given by $\text{var}(q_l) = a + bL^{-c}$. They found a finite value for a , for all the temperatures simulated, which implies $d = d_s$ and that a pure law behavior (L^{-e}) is excluded by the data. In Figure 18 the variance of the link overlap is plotted against the lattice sizes, in addition to the different fits used (to $a + b/L^c$). The same analysis on the four dimensional Ising spin glasses provides the same picture ($d = d_s$ and $\theta' = 0$). However, let us end this section recalling that it has been argued [86] that, in principle, results obtained with f.b.c show larger finite-size corrections than results obtained with p.b.c. On the other hand, f.b.c do not pose any restriction on the position of the domain wall. Hence, it is not clear if the results reported for f.b.c represent the asymptotic behavior and what are the optimal boundary conditions for this kind of studies.

8 Conclusions

We have reviewed in detail (some) recent works on finite dimensional spin glasses obtained with numerical simulations and in some cases, we have done a direct comparison with experimental results. Moreover we have tried to describe the numerical data with the competing three theoretical pictures which try to describe the low temperature phase of finite dimensional spin glasses.

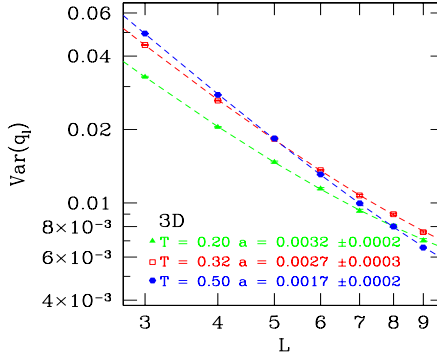


Figure 18: Log-log plot of the variance of the link overlap as a function of the size (with free boundary conditions) for different temperatures. Taken from reference [89].

Of course, as said in the introduction, we have omitted important issues (we apologize), but we hope that this review will clearly show which are the difficulties faced and the open/closed problems regarding this interesting and active field of Statistical Mechanics and Condensed Matter.

9 Acknowledgments

First of all, I warmly thank Enzo Marinari, Giorgio Parisi and Federico Ricci-Tersenghi for a long and fruitful collaboration. Moreover, I thank the people of the RTN group, with them I started to do research in Statistical Mechanics and I still maintain an interesting collaboration: José Luis Alonso, Andrés Cruz, Luis Antonio Fernández, Antonio Muñoz, Alfonso Tarancón, Sergio Jiménez, Jarda Pech, and Víctor Martín-Mayor. I thank (again) V. Martín-Mayor, Rodolfo Cuerno and Elka Korutcheva for a critical reading of the manuscript. I cannot forget Barbara Coluzzi, David Iñiguez, Paola Ranieri, Marco Ferrero, Francesco Zuliani, Daniel Stariolo, Remi Monasson, David Lancaster, Felix Ritort, Leticia Cugliandolo, Jorge Kurchan, José Carlos Ciria, Carlos L. Ullod and Hector G. Ballesteros. Finally I acknowledge financial support from the grants PB98-842, BFM2001-0718 (CICYT) and DYGLAGEMEM (European Union).

References

- [1] J. A. Mydosh, *Spin Glasses: an Experimental Introduction* (Taylor and Francis, London 1993).
- [2] W. L. McMillan, J. Phys. C **17**, 3179 (1984); A. J. Bray and M. A. Moore, in *Heidelberg Colloquium on Glassy Dynamics*, edited by J. L. Van Hemmen and I. Morgenstern (Springer Verlag, Heidelberg, 1986), p. 121; D. S. Fisher and D. A. Huse, Phys. Rev. Lett. **56**, 1601 (1986); Phys. Rev. B **38**, 386 (1988).
- [3] F. Krzakala and O. C. Martin, Phys. Rev. Lett. **85**, 3013 (2000).
- [4] M. Palassini and A. P. Young, Phys. Rev. Lett. **85**, 3017 (2000).
- [5] G. Parisi, Phys. Lett. A **73**, 203 (1979); J. Phys. A **13**, L**115** (1980); J. Phys. A **13**, 1101 (1980); J. Phys. A **13** 1887 (1980).
- [6] M. Mézard, G. Parisi and M. A. Virasoro, *Spin Glass Theory and Beyond*. World Scientific (Singapore 1987).
- [7] E. Marinari, G. Parisi, F. Ricci-Tersenghi, J. J. Ruiz-Lorenzo and F. Zuliani, J. Stat. Phys. **98**, 973 (2000).
- [8] F. Guerra, Int. J. Mod. Phys. B **10**, 1675 (1996); M. Aizenman and P. Contucci, J. Stat. Phys. **92**, 765 (1998); C. M. Newman and D. L. Stein, Phys. Rev. Lett. **76**, 4821 (1996); C. M. Newman and D. L. Stein, Phys. Rev. Lett. **76**, 515 (1996); G. Parisi, cond-mat/9603101; C. M. Newman and D. L. Stein, Phys. Rev. E **57**, 1356 (1998).
- [9] L. Berthier, J.-L. Barrat and J. Kurchan, Phys. Rev. E **63**, 016105 (2001)
- [10] D. Stariolo, Europhys. Lett. **55**, 726 (2001).
- [11] S. Ciliberti and E. Marinari, cond-mat/0304273.
- [12] G. Parisi and F. Ricci-Tersenghi, J. Phys. A, **33**, 113 (2000).
- [13] S. Franz and F. Ricci-Tersenghi, Phys. Rev. E **61**, 1121 (2000).
- [14] D. Petit, L. Fruchter and I. A. Campbell, Phys. Rev. Lett. **83**, 5130 (1999).
- [15] L. W. Lee and A.P. Young, cond-mat/0302371.
- [16] M. Picco, F. Ricci-Tersenghi and F. Ritort, Phys. Rev B **63**, 174412 (2001); Eur. Phys. J. B **21**, 211 (2001).

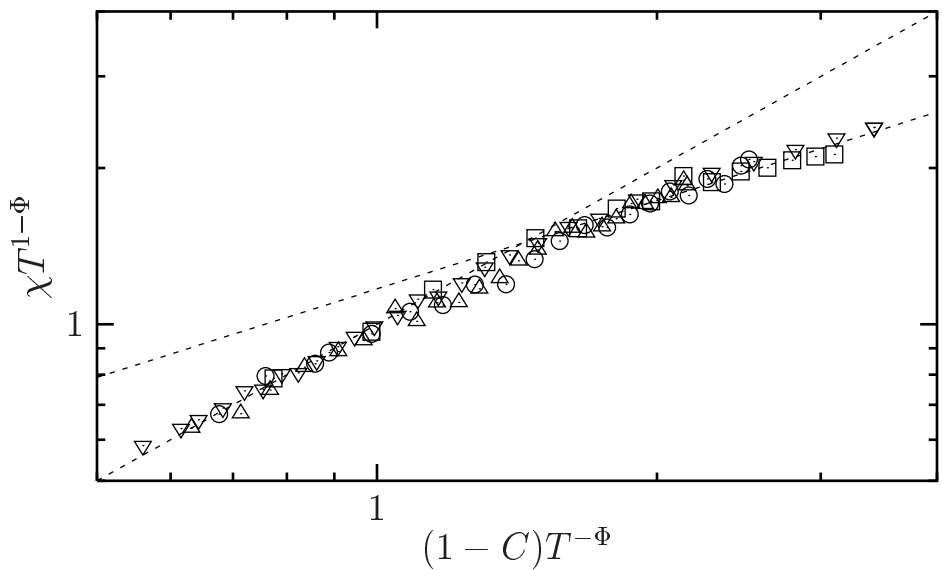
- [17] A. K. Hartmann and A. P. Young, cond-mat/0205659.
- [18] A. A. Middleton, Phys. Rev. Lett. **83**, 1672 (1999); Phys. Rev. B **63**, 060202(R) (2001).
- [19] H. Castillo *et al.*, Phys. Rev. Lett. **88**, 237201 (2002).
- [20] A. Montanari and F. Ricci-Tersenghi, Phys. Rev. Lett. **90**, 017203 (2003).
- [21] G. Parisi, cond-mat/0208070.
- [22] L. Berthier, cond-mat/0303453.
- [23] A. Billoire and B. Coluzzi, cond-mat/0210489.
- [24] A. Billoire and B. Coluzzi, cond-mat/0302026.
- [25] E. Marinari, V. Martin-Mayor and A. Pagnani, Phys. Rev. B **62**, 4999 (2000).
- [26] A. Crisanti and T. Rizzo, Phys. Rev. Lett. **90**, 137201 (2003).
- [27] A. Billoire and E. Marinari, cond-mat/0202437. To appear in Europhys. Lett.
- [28] H. Takayama and K. Hukushima, cond-mat/0205276.
- [29] T. Aspelmeier, A. J. Bray and M. A. Moore, Phys. Rev. Lett. **89**, 197202 (2002).
- [30] L. Correale, E. Marinari and V. Martín-Mayor, Phys. Rev. B **66**, 174406 (2002).
- [31] F. Krzakala and O. C. Martin, Phys. Rev. Lett. **89**, 267202 (2002).
- [32] J. Houdayer and O. C. Martin, Phys. Rev. Lett. **82**, 4934 (1999).
- [33] F. Krzakala, J. Houdayer, E. Marinari, O. C. Martin and G. Parisi, Phys. Rev. Lett. **87**, 197204 (2001).
- [34] J. Lamarcq, J.-P. Bouchaud and O. C. Martin, cond-mat/0208100.
- [35] A. Cruz, L. A. Fernandez, S. Jiménez, J. J. Ruiz-Lorenzo and A. Tarancón, cond-mat/0209350. To appear in Phys. Rev. B.
- [36] K. Binder and A. P. Young, Rev. Mod. Phys. **58**, 801 (1986).

- [37] K. H. Fisher and J. A. Hertz, *Spin Glasses* (Cambridge University Press, Cambridge, 1991).
- [38] H. Rieger, in *Annual Reviews of Computational Physics II* (World Scientific 1995, Singapore) p. 295.
- [39] E. Marinari, G. Parisi and J. J. Ruiz-Lorenzo, *Numerical Simulations of Spin Glass Systems in Spin Glasses and Random Fields*, edited by A. P. Young (World Scientific, Singapore, 1998).
- [40] K. Gunnarsson et al., Phys. Rev. B **43**, 8199 (1991). See also P. Norblad and P. Svendlidh *Experiments on Spin Glasses in Spin Glasses and Random Fields*, edited by A. P. Young (World Scientific, Singapore, 1998).
- [41] J.P. Bouchaud, L. Cugliandolo, J. Kurchan and M. Mézard, *Out of equilibrium dynamics in spin glasses and other glassy systems in Spin Glasses and Random Fields*, edited by A. P. Young (World Scientific, Singapore, 1998).
- [42] J. P. Bouchaud, cond-mat/9910387.
- [43] L. Cugliandolo, cond-mat/0210312.
- [44] A. Crisanti and F. Ritort, cond-mat/0212490.
- [45] C. de Dominicis, I. Kondor and T. Temesvári, *Beyond the Sherrington-Kirkpatrick Model in Spin Glasses and Random Fields*, edited by A. P. Young. (World Scientific, Singapore, 1998).
- [46] J. Cardy *Scaling and Renormalization in Statistical Physics* (Cambridge University Press, Cambridge, 1996) or M. N. Barber, in *Phase Transitions and Critical Phenomena*, Vol 8, edited by C. Domb and J. L. Lebowitz (Academic Press, London, 1983).
- [47] S. F. Edwards and P. W. Anderson, J. Phys. F **5**, 965 (1975).
- [48] H. G. Ballesteros, L. A. Fernández, V. Martín-Mayor, A. Muñoz Sudupe, G. Parisi and J. J. Ruiz-Lorenzo, Phys. Lett. B 400, 346 (1997); Nucl. Phys. B **512** [FS], 681 (1998) ; Phys. Rev. B **58**, 2740 (1998).
- [49] F. Cooper, B. Freedman and D. Preston, Nucl. Phys. B **210**, 210 (1989).
- [50] H. G. Ballesteros *et al.* , Phys. Rev. B **62**, 14237 (2000).
- [51] F. Ritort and M. Sales, J. Phys. A **33**, 6505 (2000).

- [52] J. Pech, A. Tarancón and C.L. Ullod, Comp. Phys. Comm. **106**, 10 (1997); A. Cruz, J. Pech, A. Tarancón, P. Téllez, C. L. Ullod and C. Ungil. *idib* **133**, 165 (2001).
- [53] J. Wang and A. P. Young, J. Phys. A **26**, 1063 (1993).
- [54] J. J. Ruiz-Lorenzo, J. Phys. A **31**, 8773 (1998).
- [55] G. Parisi, P. Ranieri, F. Ricci-Tersenghi and J. J. Ruiz-Lorenzo, J. Phys. A **30**, 7115 (1997).
- [56] G. Parisi, F. Ricci-Tersenghi and J. J. Ruiz-Lorenzo, J. Phys. A **29**, 7943 (1996)
- [57] E. Marinari, G. Parisi and J. J. Ruiz-Lorenzo, Phys. Rev. B. **58**, 14852 (1998).
- [58] E. Marinari, G. Parisi, F. Ritort and J. J. Ruiz-Lorenzo, Phys. Rev. Lett. **76**, 843 (1996).
- [59] J. Kisker, L. Santen, M. Schreckenberg and H. Rieger, Phys. Rev. B **53**, 6418 (1996).
- [60] L. Berthier and J. P. Bouchaud, Phys. Rev. B **66**, 054404 (2002).
- [61] Y. G. Joh, R. Orbach, G. G. Wood, J. Hammann and E. Vincent, Phys. Rev. Lett. **82**, 438 (1999).
- [62] J. P. Bouchaud, V. Dupuis, J. Hammann and E. Vicent, Phys. Rev. B **65**, 024439 (2002).
- [63] F. Lefloch, J. Hammann, M. Ocio and E. Vincent, Europhys. Lett. **18**, 647 (1992).
- [64] K. Jonason, E. Vincent, J. Hammann, J. P. Bouchaud and P. Norblad, Phys. Rew. Lett. **81**, 3243 (1998).
- [65] L. F. Cugliandolo and J. Kurchan, Phys. Rev. Lett. **71**, 173 (1993); Phil. Mag. **71**, 501 (1995); J. Phys. A **27**, 5749 (1994).
- [66] S. Franz and M. Mézard, Europhys. Lett. **26**, 209 (1994).
- [67] A. Baldassarri, L. F. Cugliandolo, J. Kurchan and G. Parisi, J. Phys. A **28**, 1831 (1995).
- [68] E. Marinari, G. Parisi, F. Ricci-Tersenghi and J. J. Ruiz-Lorenzo, J. Phys. A **31**, 2611 (1998).

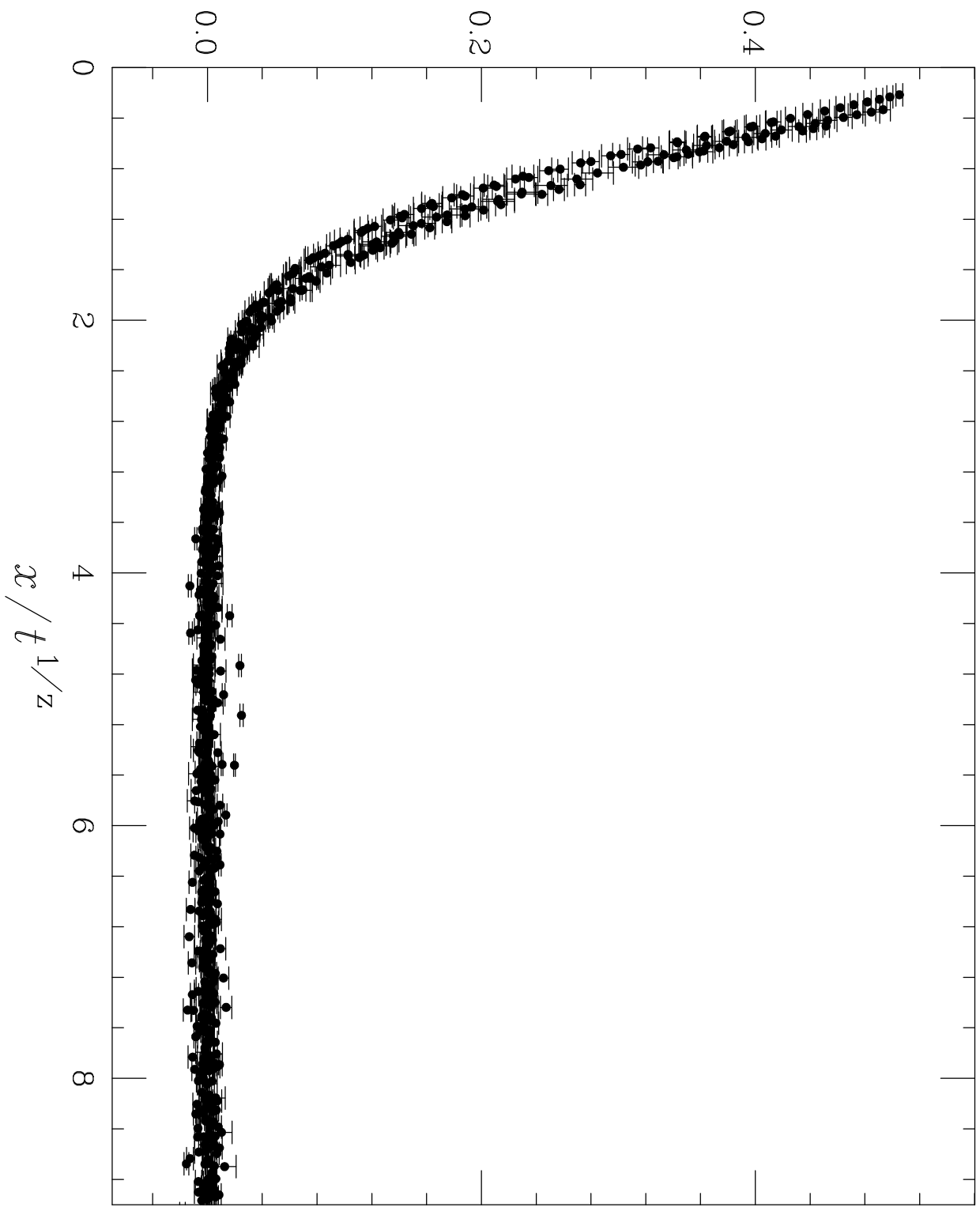
- [69] S. Franz and H. Rieger, *J. Stat. Phys.* **79**, 749 (1995).
- [70] S. Franz, M. Mézard, G. Parisi, L. Peliti, *Phys. Rev. Lett.* **81**, 1758 (1998); *J. Stat. Phys.* **97**, 459 (1999).
- [71] G. Parisi and G. Toulouse, *J. Physique Lett.* **41**, L361 (1980).
- [72] A. Crisanti, T. Rizzo and T. Temesvari, [cond-mat/0302538](https://arxiv.org/abs/cond-mat/0302538).
- [73] D. Hérisson and M. Ocio, *Phys. Rev. Lett.* **88**, 257202 (2002).
- [74] E. Marinari, G. Parisi, F. Ricci-Tersenghi and J. J. Ruiz-Lorenzo, *J. Phys. A* **33**, 2373 (2000).
- [75] D. Iñiguez, E. Marinari, G. Parisi and J. J. Ruiz-Lorenzo, *J. Phys. A* **30**, 7337 (1997).
- [76] M. Tesi, E. Janse van Resburg, E. Orlandini and S. G. Whillington, *J. Stat. Phys.* **82**, 155 (1996); K. Hukushima and K. Nemoto, *J. Phys. Soc. Jpn.* **65**, 1604 (1996).
- [77] E. Marinari, *Optimized Monte Carlo Methods* in *Lecture Notes in Physics* 501 (Springer-Verlag, Heidelberg, 1998).
- [78] A. Barrat and L. Berthier, *Phys. Rev. Lett.* **87**, 87204 (2001).
- [79] E. Marinari and G. Parisi, *Phys. Rev. B*, 62, 11677 (2000).
- [80] G. Parisi, F. Ricci-Tersenghi and J. J. Ruiz-Lorenzo, *Eur. Phys. J. B*, **10**, 317 (1999).
- [81] E. Marinari, G. Parisi, F. Ricci-Tersenghi and J. J. Ruiz-Lorenzo, *J. Phys. A* **31**, L481 (1998).
- [82] E. Marinari, G. Parisi and J. J. Ruiz-Lorenzo, *J. Phys. A* **35**, 6805 (2002).
- [83] J. Houdayer and O. C. Martin, *Europhys. Lett.* **49**, 794 (2000).
- [84] J. Houdayer, F. Krzakala and O. C. Martin, *Eur. Phys. J.* **18**, 467 (2000).
- [85] J. Houdayer and O. C. Martin, *Phys. Rev. Lett.* **81**, 2554 (1998); J. Lamarcq, J.-P. Bouchaud, O. C. Martin and M. Mézard, *Europhys. Lett.* **58**, 321 (2002); J.-P. Bouchaud, F. Krzakala and O.C. Martin, [cond-mat/0212070](https://arxiv.org/abs/cond-mat/0212070); J. Lamarcq, J.-P. Bouchaud and O. C. Martin, [cond-mat/0208100](https://arxiv.org/abs/cond-mat/0208100).
- [86] M. Palassini, F. Liers, M. Jünger and A. P. Young, [cond-mat/0212551](https://arxiv.org/abs/cond-mat/0212551).

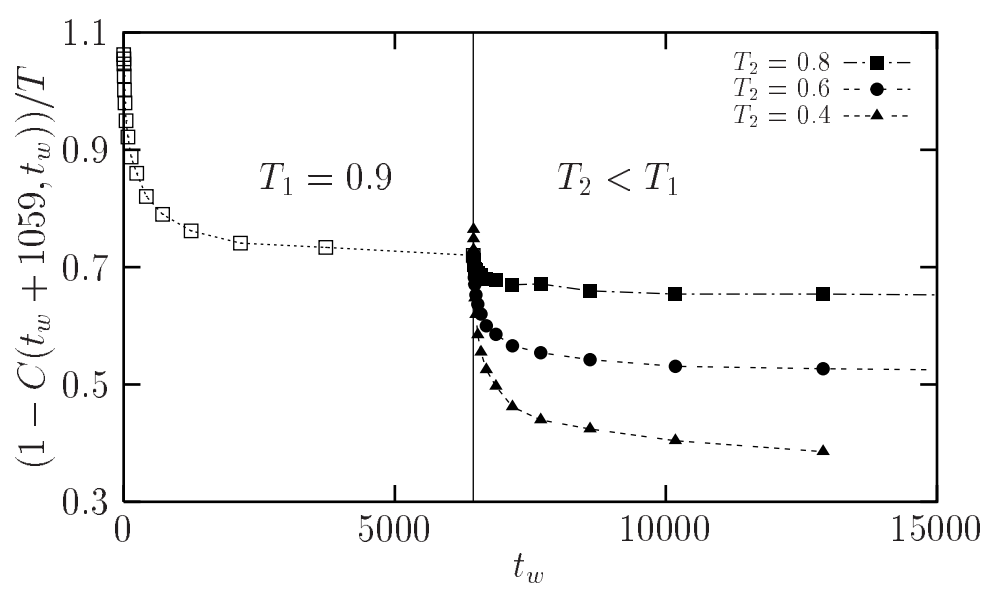
- [87] E. Marinari and G. Parisi, Phys. Rev. Lett. **86**, (2001) 3887.
- [88] H. G. Katzgraber, M. Palassini and A. P. Young, Phys. Rev. B **63**, 184422 (2001).
- [89] H. G. Katzgraber and A. P. Young, Phys. Rev. B **65**, 214402 (2002).



$$x^{0.5} C(x)$$

$L=64$





A Sample Document

Your Name Your coauthor

February 21, 2003

\LaTeX is one of the most widely used \TeX macros. This is a sample \LaTeX input file, which you can then use as a template in order to compose your contribution. Compile it twice in order to get all cross-references right. This particular document uses \LaTeX ’s “article” document style.

1 Text and Typestyles

The ends of words and sentences are marked by spaces. It doesn’t matter how many spaces you type; the end of a line counts as a space. One or more blank lines denote the end of a paragraph. \LaTeX commands are usually preceded with a backslash. They are often also included in brackets, as shown in this file. The \LaTeX command generates the \LaTeX logo. Quotation marks are usually done like “this.” Dashes come in three sizes: an intra-word dash, a medium dash for number ranges like 1–2, and a punctuation dash—like this. Should you want to cause some text to appear in **boldface type**, you can simply place the \bfseries command before that text. Should you want a sentence to appear in *italics*, you can simply use the \itshape command. *This sentence appears in italics.* You can also use different commands to cause text to appear in larger type. This paragraph uses \LaTeX ’s “large” typestyle. \LaTeX interprets some common characters as commands, so you must type special commands to generate them. These characters include the following: $\$$ & $\%$ $\#$ $\{$ and $\}$. Footnotes¹ are easy to do with \LaTeX . \LaTeX is also very good at typesetting mathematical formulas like: $x - 3y = 7$ or $a_1 > x^{2n} / y^{2n} > x'$.

¹This is an example of a footnote.

2 Displayed Math

Mathematical formulas may be placed within paragraphs of text. But they may also be “displayed.” In displayed math formulas, the formulas are displayed between lines of text, as shown below:

$$x' + y^2 = z_i^2$$

3 Lists

The following is an example of an *itemized* list.

- This is the first item of an itemized list.
- This is the second item in the list.
 1. This is the first item of an enumerated list that is nested within the itemized list.
 2. This is the second item of the inner list.
- This is the third item of the list.

4 Figures

You can use the following step by step guide to include a picture into your document using this template:

1. Export the picture from your graphics program in EPS format.
2. Use the command

```
\includegraphics[key=value, ...]{file.eps}
```

to include `file.eps` into your document. The optional parameter accepts a comma separated list of keys and associated values. The keys can be used to alter the width, height and rotation of the included graphic. The most important keys can be found in the Table. Use the lines (in the template file!) defining the Table as a template for creating your own tables.

Please, find in the template file how Fig. 1 (file `test.eps`) was included. The graphic is scaled to a final width which is 0.5 times the width of a standard paragraph, and to a final height which is 0.3 times the height of a standard paragraph.

<code>width</code>	scale graphic to the specified width
<code>height</code>	scale graphic to the specified height
<code>angle</code>	rotate graphic counterclockwise
<code>scale</code>	scale graphic

Table 1: Key Names for `graphicx` Package.



Figure 1: A sample figure

5 Bibliography

You can produce a bibliography with the `thebibliography` environment. Each entry starts with

```
\bibitem[label]{marker}
```

The marker is then used to cite the book, article or paper within the document using

```
\cite{marker}
```

If you do not use the *label* option, the entries will get enumerated automatically. The parameter after the

```
\begin{thebibliography}
```

command defines how much space to reserve for the number or labels. In the example below,

```
{ 9 }
```

tells `LATEX` to expect that none of the bibliography item numbers will be wider than the number 9. Please, find in the References section below examples on the format to be employed for the various types of references. Note that footnotes are **not** to appear among the references, but should rather be written using the

```
\footnote
```

command as explained above.

References

- [1] S. J. Brodsky and R. W. Brown, Phys. Rev. Lett. **49**, 966 (1982).
- [2] T. Sun, B. Morin, H. Guo, and M. Grant, in *Surface Disordering: Growth, Roughening and Phase Transitions*, edited by R. Jullien *et al.* (Nova Science, New York, 1992).
- [3] S. A. Safran, *Statistical Thermodynamics of Surfaces, Interfaces, and Membranes* (Addison Wesley, Reading, MA, 1994).
- [4] E. Pauné, Ph.D. thesis, Universitat de Barcelona, 2002.
- [5] A. A. Clerk, S. M. Girvin, and A. D. Stone, preprint cond-mat/0211001.

